

# Multifunctional Nanoworms and Nanorods through a One-Step Aqueous Dispersion Polymerization

Zhongfan Jia, Valentin A. Bobrin, Nghia P. Truong, Marianne Gillard, and Michael J. Monteiro\*

Australian Institute for Bioengineering and Nanotechnology, The University of Queensland, St Lucia, Brisbane QLD 4072, Australia

**S** Supporting Information

**ABSTRACT:** Producing synthetic soft worm and rod structures with multiple chemical functionalities on the surface would provide potential utility in drug delivery, nanoreactors, tissue engineering, diagnostics, rheology modifiers, enzyme mimics, and many other applications. Here, we have synthesized multifunctional worms and rods directly in water using a one-step reversible addition–fragmentation chain transfer (RAFT)-mediated dispersion polymerization at high weight fractions of polymer (>10 wt %). The chain-end functionalities included alkyne, pyridyl disulfide, dopamine,  $\beta$ -thiolactone, and biotin groups. These groups could further be converted or coupled with biomolecules or polymers. We further demonstrated a nanorod colorimetric system with good control over the attachment of fluorescent probes.

Multifunctional nanostructures, including spheres, vesicles, worms and rods, surface functionalized with combinations of biological molecules (e.g., siRNA, peptides, enzymes), prodrugs, imaging agents, and other molecules have generated intense interest for a wide variety of applications.<sup>1</sup> Long and flexible worms have *in vivo* blood circulation times about 10 times longer than their spherical analogues<sup>2</sup> and have been found to have significantly longer circulation times than any synthetic particle or PEO-coated stealth vesicles.<sup>3</sup> Short rods, on the other hand, have much shorter circulations times but are more efficiently taken up by cells.<sup>2</sup> This together with the excellent *in vivo* antitumor activity<sup>3</sup> demonstrate the great potential of worms and rods in nanomedicine. The unique properties of worms and rods is not surprising as nature has produced the well-known cylindrical biostructured viruses to elude the body's immune system, which include the worm-like Potato Virus Y (PVY)<sup>4</sup> and rod-like Tobacco Mosaic Virus (TMV).<sup>5</sup> Worms have further attracted interest due to their high aspect ratio to alter the rheology<sup>6</sup> and gelation properties of materials.<sup>7</sup>

The most utilized method to prepare worms is through the self-assembly of amphiphilic diblock copolymer, starting from a good solvent for both blocks followed by the slow addition of water (a poor solvent for hydrophobic block) until reaching the required solvent ratio.<sup>8</sup> The worms are cross-linked either in the core or shell<sup>9</sup> depending upon the application<sup>10</sup> and extensively dialyzed with water to remove any organic solvent and unreacted cross-linker. This method has allowed chemical functionality on the surface of spheres and other structures for coupling with sugars, folic acid, oligonucleotides, and other biomolecules.<sup>11</sup> Worms and rods can also be prepared from dendronized

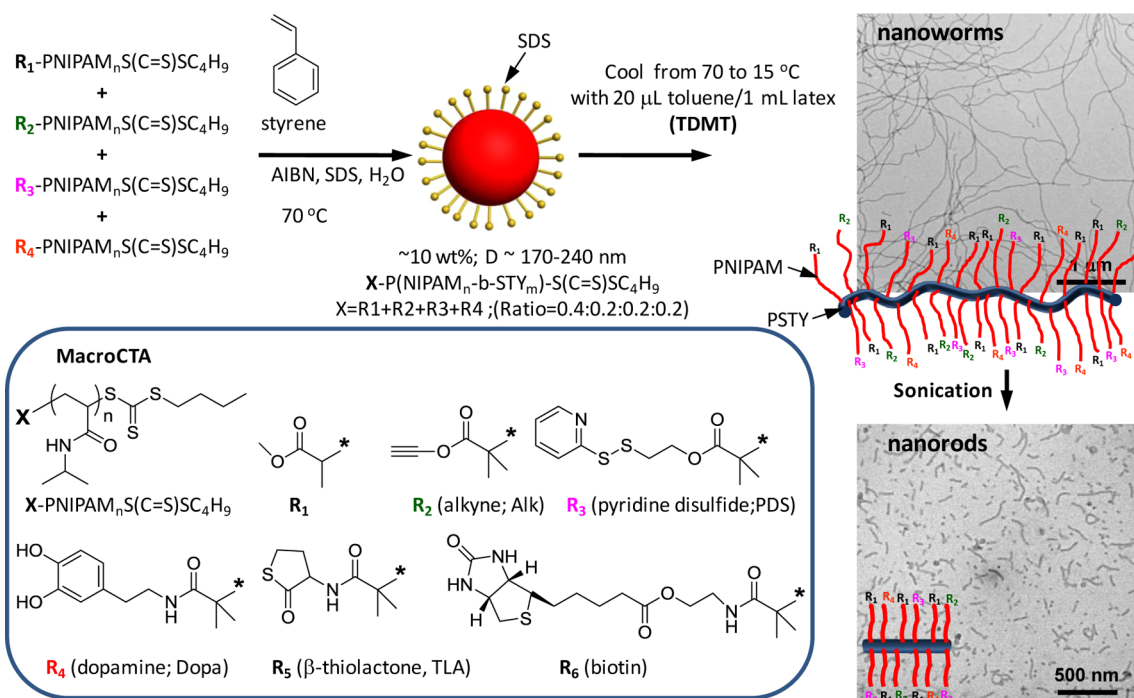
polymers with controlled diameters and lengths.<sup>12</sup> Although the self-assembly technique has found potential in many biomedical and other applications, the technique requires considerable time to produce the nanostructure of choice, the chemical functionality at the surface can become buried within the shell during the cross-linking procedure, the weight fraction of polymer is  $\sim 0.5$  wt %, and each chain-end functional polymer must be separately synthesized<sup>13</sup> which can influence the self-assembly process. Currently, there is no direct polymerization procedure to create stable worms and rods directly in water at high weight fractions of polymer with multifunctional and orthogonal chemical groups on the surface through a one-step process. Producing such nanostructures directly in water at weight fractions of 10–20 wt % would provide a facile method to covalently attach bio- and other molecules that mimic features of natural systems (e.g., worm- and rod-like viruses) and, therefore, significantly broaden the potential of such nanostructures as drug,<sup>14</sup> siRNA<sup>15</sup> and vaccine<sup>16</sup> delivery vehicles, organic photonics,<sup>17</sup> diagnostics, nanoreactors to self-healing coatings.<sup>18</sup>

Herein, we report a method to produce multifunctional worms directly in water using a one-step reversible addition–fragmentation chain transfer (RAFT)-mediated dispersion polymerization (Scheme 1). End-group functional poly(*N*-isopropylacrylamide) (PNIPAM) thermoresponsive MacroCTAs in the presence of styrene (STY), AIBN, and SDS were first assembled in water at 70 °C (i.e., well above their lower critical solution temperature (LCST) of PNIPAM) and polymerized for 3.5 h to form diblock copolymers of PNIPAM and PSTY at a weight fraction of 10 wt %. The latex solution was cooled to 23 °C (i.e., below the LCST), at which temperature the PNIPAM blocks became water-soluble, transforming the spherical structures into multifunctional nanoworms with a diameter of  $\sim 15$  nm and lengths ranging between 2 and 5  $\mu\text{m}$  in the presence of toluene (20  $\mu\text{L}$  per 1 mL of latex solution) as plasticizer. The advantage of this process is that the multifunctional chemical groups are located at the surface of the structures, maximizing further chemical transformations and coupling reactions. This technique, denoted as the temperature-directed morphology transformation (TDMT), has allowed a wide range of nanostructures to be produced,<sup>19</sup> ranging from spheres, worms, vesicles, donuts, and lamella sheets; structures that were not only stable in water for long periods of time (e.g., the worms were stable for a year at room temperature) but also could be freeze-dried and rehydrated without structural reorganization.

Received: January 8, 2014

Published: February 4, 2014

Scheme 1. Synthesis of Multifunctional Nanoworms and Nanorods Through RAFT-Mediated Emulsion Polymerization in Water Followed by TDMT and Ultrasound Cutting



Six chain-end functional RAFT agents were synthesized through modification of the carboxylic acid group of the trithiolcarbonate RAFT agent, 2-(((butylthio)carbonothioyl)-thio)-2-methylpropanoic acid (see Experimental in SI). The functional groups chosen here consisted of an alkyne (Alk) for the copper catalyzed alkyne–azide cycloaddition (CuAAC) ‘click’ reaction,<sup>20</sup> pyridyl disulfide (PDS) for thiol–disulfide exchange or thiol–ene reactions,<sup>21</sup> dopamine (Dopa) for specific binding to metal surface,<sup>22</sup> β-thiolactone (TLA) for amination reaction<sup>23</sup> and biotin for binding to streptavidin.<sup>24</sup> The RAFT-mediated polymerization of these RAFT agents with NIPAM produced six functional MacroCTAs with number-average molecular weights ( $M_n$ 's) ranging from 5100 to 5510 (i.e., with ~44 repeating units) as determined by  $^1\text{H}$  NMR and with polydispersity indexes ( $\text{PDI}_{\text{SEC}}$ 's) all below 1.12 (see Table S1, SEC chromatograms and  $^1\text{H}$  NMR spectra in SI), suggesting excellent control over the molecular weight distribution (MWD) and maintenance of high chain-end fidelity.

The first RAFT-mediated dispersion polymerization consisted of mixing four different MacroCTAs (i.e.,  $R_1$ ,  $R_2$ ,  $R_3$ , and  $R_4$  in Scheme 1 at a ratio of 0.4:0.2:0.2:0.2) with styrene, SDS, and AIBN at 70 °C (Table S2, expt 7). After a polymerization time of ~3.5 h (~75% conversion), the resultant emulsion produce polymer particles measured at 70 °C with an average number-average diameter ( $D_h$ ) of 210 nm and a variance (i.e.,  $\text{PDI}_{\text{DLS}}$ ) of 0.115, suggesting a relatively narrow particle size distribution. The MWD of the resultant polymers was well-controlled with  $M_n$  close to the theoretically calculated value and with a  $\text{PDI}_{\text{SEC}}$  of 1.10. The excellent control over the MWD further suggested high chain-end fidelity (see SEC chromatograms in SI). A small amount of toluene (20 µL per 1 mL of latex solution) was added and immediately cooled to 15 °C. The toluene was added to plasticize the glassy PSTY and aid in the temperature-directed morphology transformation. Long and flexible worms formed consisting of a PSTY core and a PNIPAM hairy layer, in which

the functional groups were located at the PNIPAM chain-ends (see Scheme 1 for transmission electron micrograph (TEM) of the worms). We then utilized the Winnik et al.<sup>25</sup> ultrasound method to cut the worms to short rods with an approximate length of 150 nm and the same core diameter (see TEM in Scheme 1 and histogram in Figure S18). Our ultrasound conditions for the cutting of worms supported the theory of Winnik et al.<sup>25</sup> that the limiting rod size was 100 nm (see Figure S19). Our procedure demonstrates the ease of producing worms and rods with many different functional groups on the surface via a one-step polymerization directly in water and at high weight fractions of polymer. NMR analysis of this and the following block copolymers were freeze-dried to remove all water and low boiling point compounds and then dissolved in  $\text{CDCl}_3$ , and for SEC analysis a small amount of latex was dissolved in THF and directly injected into the SEC system.

The next polymerization (Table S2, expt 1) used 100% of the alkyne MacroCTA ( $R_2$ ) to produce a narrow particle size distribution ( $D_h = 189$  nm and  $\text{PDI}_{\text{DLS}} = 0.067$ ) and narrow MWD ( $M_n = 8500$ ,  $\text{PDI}_{\text{SEC}} = 1.14$ ). Using the same TDMT procedure above, the spherical latex particles were transformed to worms and then cut to short rods using ultrasound (see Figure S17), in which each PNIPAM chain-end consisted of a reactive alkyne moiety (Figure 1A). The worms and rods were coupled through the CuAAC ‘click’ reaction with PNIPAM- $\text{N}_3$  and PEG- $\text{N}_3$ , (see SI for experimental and characterization details for these azide functional polymers). The coupling efficiency determined by  $^1\text{H}$  NMR for PNIPAM- $\text{N}_3$  ( $M_n = 4340$ ,  $\text{PDI}_{\text{SEC}} = 1.06$ ) and PEG- $\text{N}_3$  ( $M_n = 2800$ ,  $\text{PDI}_{\text{SEC}} = 1.10$ ) to the long worms was 88 and 82%, respectively, and coupling efficiency to the short rods was slightly higher at 86 and 90%, respectively. Heating these worm and rod solutions above the LCST (~37 °C) of the PNIPAM block produced a gel that when cooled dissociated back to a sol; a process that is fully reversible (Figure 1B depicting the gel–sol transformation). The alkyne functional

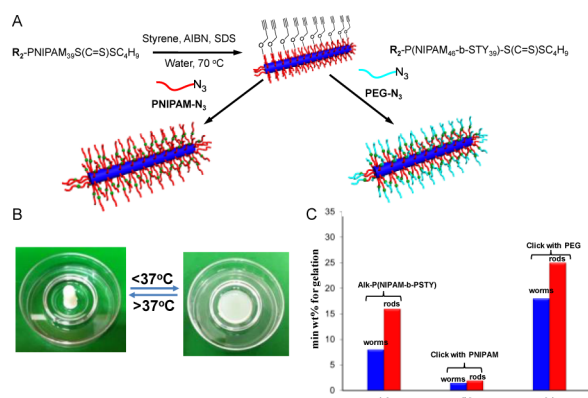


**Figure 1.** (A) Schematic showing the modification of 100% alkyne functional worms and rods  $R_1$ -P(NIPAM<sub>45</sub>-*b*-STY<sub>39</sub>) (Table S2, expt 1) through CuAAC ‘click’ reaction. (B) Photos showing the typical gel–sol transformation. (C) Minimum weight percentage of gel formation at 37 °C: (a)  $R_1$ -P(NIPAM<sub>45</sub>-*b*-STY<sub>39</sub>), (b) P(NIPAM<sub>43</sub>-*b*-NIPAM<sub>45</sub>-*b*-STY<sub>39</sub>), and (c) P(EG<sub>45</sub>-*b*-NIPAM<sub>45</sub>-*b*-STY<sub>39</sub>); blue bar for worms and red bar for rods.

worms and rods formed gels at a minimum weight fraction of 8 and 16 wt %, respectively (Figure 1C). Coupling PNIPAM-N<sub>3</sub> significantly reduced the minimum wt% for gelation to 1.5 and 2 wt % for the worms and rods, respectively. This suggests that above the LCST, the higher molecular weight of the second PNIPAM block resulted in greater interworm interaction thus significantly lowering the gel point. On the other hand, coupling PEG-N<sub>3</sub> increased the gel point, most probably due to the decreased interactions between the worms or rods. This level of control over the gel properties together with the variety of chemical groups has the potential as scaffolds for tissue engineering.

Other functional worms and rods were produced using the TDMT method with pyridyl disulfide (PDS) or  $\beta$ -thiolactone (Tla) end groups (Table S2, expts 2 and 4). Pyridyl disulfide has been widely used in conjugation reactions of polymers and biomolecules with sugar,<sup>26</sup> peptides,<sup>27</sup> oligonucleotides,<sup>28</sup> proteins,<sup>29</sup> and anticancer drugs.<sup>30</sup> The worms and rods with PDS (Table S2, expt 2) were prepared from an equal ratio of MacroCTAs,  $R_1$ , and  $R_3$ . The MWD was again well-controlled, and the worms and rods then characterized by TEM (Figure S17). The PDS-worms and PDS-rods were further reacted with the model peptide that is reduced L-glutathione (GSH, 5 equiv to PDS groups) to produce peptide surface coated worms and rods (Figure 2A). The excess of GSH was easily dialyzed out. The conjugation efficiency to the nanorods was also measured by UV–vis absorbance of 2-mercaptopyridine released after coupling, giving a conjugation efficiency of 79%, which was supported by the conjugation efficiency determined by <sup>1</sup>H NMR of 75% (through the loss of the pyridyl disulfide). The conjugation efficiency was slightly lower for the worms (Figure 2B). In the case of the Tla worms and rods, we ring-opened the thiolactone with allylamine and subsequently protected the resultant free thiol using dipyridyl disulfide (DPDS) to form pyridyl disulfide and alkene functional worms and rods in a one-pot reaction (Figure 2C), allowing for the possibility of further sequential reactions. The coupling efficiency with allylamine was 81% for worms and 95% for rods (see Table S4). The GSH and allylamine are highly water soluble and should be effectively dialyzed out before NMR or UV analysis. In addition, allylamine has a low boiling point and will be removed after freeze drying.

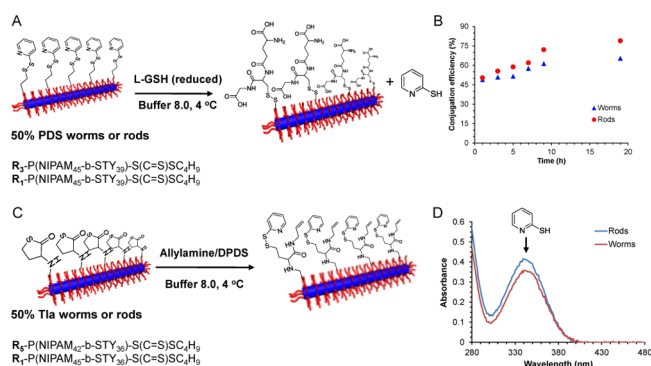


**Figure 2.** (A) Schematic showing the modification of 50% PDS functional nanoworms and nanorods (Table S2, expt 2) with L-glutathione (GSH). (B) Conjugation efficiency vs time for worm (blue triangle) and rods (red circle) from the UV–vis spectra of released 2-mercaptopyridine after the conjugation of GSH with PDS functional nanoworms and nanorods, respectively; the molar ratio of GSH to PDS was 5. (C) Schematic showing the modification of 50% Tla functional nanoworms and nanorods (Table S2, expt 4) with allylamine and DPDS. (D) UV–vis spectra showing the release of 2-mercaptopyridine for the reaction of nanoworms (dark-red line) and nanorods (light-blue line) with allylamine and DPDS.

Taken together, the results demonstrate the efficient coupling due to the location of the functional end groups extending from the surface of the worms and rods well into the water phase.

To test the level of control over the percentage of functional groups on the surface, we used three MacroCTAs ( $R_1$ ,  $R_3$ , and  $R_6$ ) to produce rods with different ratios of functional groups (Table S2, expts 8–10) as shown in Figure 3. The rods were then

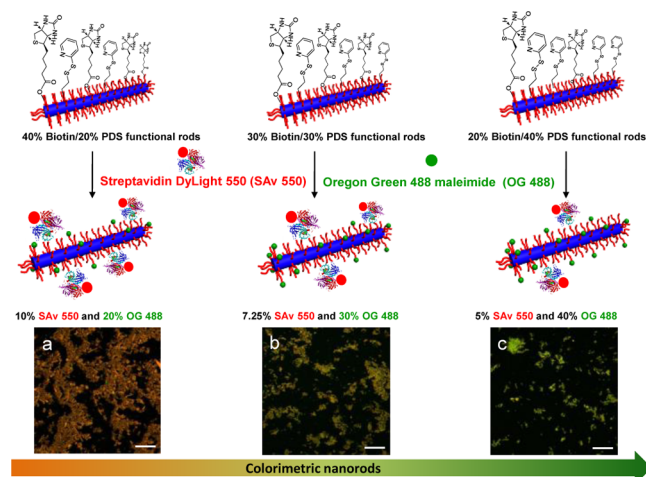


**Figure 3.** Stoichiometric bioorthogonal conjugation of PDS and biotin functional groups on the nanorods (Table S2, expts 8–10) with maleimide functional Oregon green 488 and Streptavidin DyLight 550, respectively. The ratio of SAv DyLight 550 to biotin was 1:4 and Oregon green 488 maleimide to PDS was 1:1; (a–c) showing the colorimetric change of nanorods after functionalization.

coupled through the PDS ( $R_3$ ) groups with the fluorescence Oregon green 488 maleimide (1 equiv to PDS groups) and the rods then further coupled with Streptavidin DyLight 550 (SAv 550) (0.25 equiv to biotin ( $R_6$ ) groups since there are four binding sites on SAv 550). Confocal microscopy of the merged image from the 488 and 550 nm channels showed that as the biotin ratio to PDS was reduced from 2 to 0.5; the image changed

from orange to yellow to green in accord with the expected ratio of Oregon green to SA<sub>v</sub> 550. This supports the generation of nanorods with qualitative stoichiometric chemical functionality on the surface, resulting in the production of a series of colorimetric rods for potential application in diagnostic assays.

In conclusion, we have demonstrated a technique to directly prepare worms and rods in water at a weight fraction of 10 wt % with a multifunctional surface. In one example, we were able to couple four different function groups to produce worms and rods in which the diblock copolymer chains were of a narrow molecular weight distribution. Other functional worms and rods with alkyne, pyridyl disulfide, and biotin allowed further attachment of polymers, peptides, and fluorescence molecules. The  $\beta$ -thiolactone functional worms and rods were converted to difunctional end groups for further orthogonal reactions. We believe that this methodology of producing multifunctional worms and rods will have utility in drug delivery, nanoreactors, tissue engineering, diagnostics, rheology modifiers, enzyme mimics, and many other applications.

## ■ ASSOCIATED CONTENT

### ■ Supporting Information

Materials, synthetic procedures, characterization of compounds and polymers. This material is available free of charge via the Internet at <http://pubs.acs.org>.

## ■ AUTHOR INFORMATION

### Corresponding Author

m.monteiro@uq.edu.au

### Notes

The authors declare no competing financial interest.

## ■ ACKNOWLEDGMENTS

Australian Research Council (ARC) Discovery grant.

## ■ REFERENCES

- (1) (a) Hubbell, J. A.; Chilkoti, A. *Science* **2012**, *337*, 303. (b) Liu, X. H.; Jin, X. B.; Ma, P. X. *Nat. Mater.* **2011**, *10*, 398. (c) O'Reilly, R. K.; Hawker, C. J.; Wooley, K. L. *Chem. Soc. Rev.* **2006**, *35*, 1068.
- (2) Geng, Y.; Dalhaimer, P.; Cai, S.; Tsai, R.; Tewari, M.; Minko, T.; Discher, D. E. *Nat. Nanotechnol.* **2007**, *2*, 249.
- (3) Cai, S. S.; Vijayan, K.; Cheng, D.; Lima, E. M.; Discher, D. E. *Pharm. Res.* **2007**, *24*, 2099.
- (4) (a) Dougherty, W. G.; Carrington, J. C. *Annu. Rev. Phytopathol.* **1988**, *26*, 123. (b) Riechmann, J. L.; Lain, S.; Garcia, J. A. *J. Gen. Virol.* **1992**, *73*, 1.
- (5) (a) Klug, A. *Philos. Trans. R. Soc., B* **1999**, *354*, 531. (b) Namba, K.; Stubbs, G. *Science* **1986**, *231*, 1401.
- (6) (a) Oelschlaeger, C.; Waton, G.; Candau, S. J. *Langmuir* **2003**, *19*, 10495. (b) Dreiss, C. A. *Soft Matter* **2007**, *3*, 956. (c) Cardiel, J. J.; Dohnalkova, A. C.; Dubash, N.; Zhao, Y.; Cheung, P.; Shen, A. Q. *P. Natl. Acad. Sci. U.S.A.* **2013**, *110*, E1653. (d) Zhang, W.; Charleux, B.; Cassagnau, P. *Macromolecules* **2012**, *45*, 5273.
- (7) (a) Huang, Z.; Lee, H.; Lee, E.; Kang, S.-K.; Nam, J.-M.; Lee, M. *Nat. Commun.* **2011**, *2*, 459. (b) Zhang, S. M.; Greenfield, M. A.; Mata, A.; Palmer, L. C.; Bitton, R.; Mantei, J. R.; Aparicio, C.; de la Cruz, M. O.; Stupp, S. I. *Nat. Mater.* **2010**, *9*, 594. (c) Groison, E.; Brusseau, S.; D'Agosto, F.; Magnet, S.; Inoubli, R.; Couvreur, L.; Charleux, B. *ACS Macro Lett.* **2012**, *1*, 47. (d) Blanzas, A.; Verber, R.; Mykhaylyk, O. O.; Ryan, A. J.; Heath, J. Z.; Douglas, C. W. I.; Armes, S. P. *J. Am. Chem. Soc.* **2012**, *134*, 9741.
- (8) (a) Mai, Y. Y.; Eisenberg, A. *Chem. Soc. Rev.* **2012**, *41*, 5969. (b) Discher, B. M.; Won, Y. Y.; Ege, D. S.; Lee, J. C. M.; Bates, F. S.; Discher, D. E.; Hammer, D. A. *Science* **1999**, *284*, 1143.

- (9) (a) Guo, A.; Liu, G. J.; Tao, J. *Macromolecules* **1996**, *29*, 2487. (b) Thurmond, K. B.; Kowalewski, T.; Wooley, K. L. *J. Am. Chem. Soc.* **1996**, *118*, 7239.
- (10) Elsabahy, M.; Wooley, K. L. *J. Polym. Sci., Polym. Chem.* **2012**, *50*, 1869.
- (11) (a) Joralemon, M. J.; Murthy, K. S.; Remsen, E. E.; Becker, M. L.; Wooley, K. L. *Biomacromolecules* **2004**, *5*, 903. (b) Pan, D. J.; Turner, J. L.; Wooley, K. L. *Chem. Commun.* **2003**, 2400. (c) Pan, D. J.; Turner, J. L.; Wooley, K. L. *Macromolecules* **2004**, *37*, 7109. (d) Liu, H.; Jiang, X. Z.; Fan, J.; Wang, G. H.; Liu, S. Y. *Macromolecules* **2007**, *40*, 9074. (e) Nystrom, A. M.; Wooley, K. L. *Tetrahedron* **2008**, *64*, 8543. (f) Zhang, L.; Nguyen, T. L. U.; Bernard, J.; Davis, T. P.; Barner-Kowollik, C.; Stenzel, M. H. *Biomacromolecules* **2007**, *8*, 2890.
- (12) (a) Percec, V.; Ahn, C. H.; Ungar, G.; Yearley, D. J. P.; Moller, M.; Sheiko, S. S. *Nature* **1998**, *391*, 161. (b) Percec, V.; Ahn, C. H.; Cho, W. D.; Jamieson, A. M.; Kim, J.; Leman, T.; Schmidt, M.; Gerle, M.; Moller, M.; Prokhorova, S. A.; Sheiko, S. S.; Cheng, S. Z. D.; Zhang, A.; Ungar, G.; Yearley, D. J. P. *J. Am. Chem. Soc.* **1998**, *120*, 8619. (c) Rosen, B. M.; Wilson, C. J.; Wilson, D. A.; Peterca, M.; Imam, M. R.; Percec, V. *Chem. Rev.* **2009**, *109*, 6275. (d) Peterca, M.; Percec, V.; Leowanawat, P.; Bertin, A. *J. Am. Chem. Soc.* **2011**, *133*, 20507. (e) Kakwere, H.; Perrier, S. *J. Am. Chem. Soc.* **2009**, *131*, 1889.
- (13) (a) Twaites, B.; Alarcon, C. D.; Alexander, C. *J. Mater. Chem.* **2005**, *15*, 441. (b) Hu, J. M.; Liu, S. Y. *Macromolecules* **2010**, *43*, 8315. (c) Li, C. H.; Hu, J. M.; Liu, S. Y. *Soft Matter* **2012**, *8*, 7096. (d) Li, C. H.; Liu, S. Y. *Chem. Commun.* **2012**, *48*, 3262. (e) Langer, R.; Tirrell, D. A. *Nature* **2004**, *428*, 487.
- (14) (a) Gu, W. Y.; Jia, Z. F.; Truong, N. P.; Prasad, I.; Xiao, Y.; Monteiro, M. J. *Biomacromolecules* **2013**, *14*, 3386. (b) Truong, N. P.; Gu, W. Y.; Prasad, I.; Jia, Z. F.; Crawford, R.; Xiao, Y.; Monteiro, M. J. *Nat. Commun.* **2013**, *4*, 1902.
- (15) (a) Skwarczynski, M.; Zaman, M.; Urbani, C. N.; Lin, I. C.; Jia, Z.; Batzloff, M. R.; Good, M. F.; Monteiro, M. F.; Toth, I. *Angew. Chem., Int. Ed.* **2010**, *49*, 5742. (b) Liu, T. Y.; Hussein, W. M.; Jia, Z. F.; Ziora, Z. M.; McMillan, N. A. J.; Monteiro, M. J.; Toth, I.; Skwarczynski, M. *Biomacromolecules* **2013**, *14*, 2798.
- (16) Huynh, W. U.; Dittmer, J. J.; Alivisatos, A. P. *Science* **2002**, *295*, 2425–2427.
- (17) (a) Monteiro, M. J. *Macromolecules* **2010**, *43*, 1159. (b) Monteiro, M. J.; Cunningham, M. F. *Macromolecules* **2012**, *45*, 4939.
- (18) (a) Kessel, S.; Urbani, C. N.; Monteiro, M. J. *Angew. Chem., Int. Ed.* **2011**, *50*, 8082. (b) Kessel, S.; Truong, N. P.; Jia, Z. F.; Monteiro, M. J. *J. Polym. Sci., Polym. Chem.* **2012**, *50*, 4879. (c) Jia, Z. F.; Truong, N. P.; Monteiro, M. J. *Polym. Chem.* **2013**, *4*, 233.
- (19) Zhang, S.; Li, Z.; Samarajeewa, S.; Sun, G.; Yang, C.; Wooley, K. L. *J. Am. Chem. Soc.* **2011**, *133*, 11046.
- (20) Jia, Z.; Wong, L.; Davis, T. P.; Bulmus, V. *Biomacromolecules* **2008**, *9*, 3106.
- (21) Lee, H.; Dellatore, S. M.; Miller, W. M.; Messersmith, P. B. *Science* **2007**, *318*, 426.
- (22) Espeel, P.; Goethals, F.; Du Prez, F. E. *J. Am. Chem. Soc.* **2011**, *133*, 1678.
- (23) Jia, Z.; Liu, J.; Boyer, C.; Davis, T. P.; Bulmus, V. *Biomacromolecules* **2009**, *10*, 3253.
- (24) Wang, X. S.; Guerin, G.; Wang, H.; Wang, Y. S.; Manners, I.; Winnik, M. A. *Science* **2007**, *317*, 644.
- (25) Vazquez-Dorbatt, V.; Tolstyka, Z. P.; Chang, C.-W.; Maynard, H. D. *Biomacromolecules* **2009**, *10*, 2207.
- (26) van der Vlies, A. J.; O'Neil, C. P.; Hasegawa, U.; Hammond, N.; Hubbell, J. A. *Bioconjugate Chem.* **2010**, *21*, 653.
- (27) Cavalieri, F.; Ng, S. L.; Mazzuca, C.; Jia, Z. F.; Bulmus, V.; Davis, T. P.; Caruso, F. *Small* **2011**, *7*, 101.
- (28) Boyer, C.; Bulmus, V.; Liu, J.; Davis, T. P.; Stenzel, M. H.; Barner-Kowollik, C. *J. Am. Chem. Soc.* **2007**, *129*, 7145.
- (29) Hartgerink, J. D.; Beniash, E.; Stupp, S. I. *Science* **2001**, *294*, 1684.